

Application Note



ACT 5028 Resolver-To-Digital Converter

Heavy-Ion Irradiation Test Results for the ACT5028 Resolver-to-Digital Converter

**by Nathan Nowlin, Steve McEndree, Joseph Benedetto
Mission Research Corporation, Microelectronics Division**

**Daryl Butcher
Technology Applications Group**

August 2003

Released with authors permission

Heavy-Ion Irradiation Test Results for the Resolver-to-Digital Converter

Nathan Nowlin, Steve McEndree, Joseph Benedetto
Mission Research Corporation, Microelectronics Division

Daryl Butcher
Technology Applications Group

August 2003

Objectives:

1. Perform initial screening tests for device latchup.
2. Perform initial screening tests for upset rates and obtain an estimate of single-event-upset error rates.

Beam Source:

Ion-beam source time was obtained from the Brookhaven National Laboratories (BNL) Tandem Van-de-Graaf (TVDG) Accelerator Facility on July 14, 2003. All testing was done with the RDC configured in 16-bit mode.

SEL (Single-Event-Latchup) Test Results

One part (in a 52-pin LCC package) was tested for evidence of single event latchup. A ceramic strip heater was attached to the backside of the package and the temperature was controlled with a MINCO temperature controller through a feedback thermocouple. We also used a Fluke temperature sensor to further confirm the device temperature. The device was irradiated while heated to 125C and powered with a power-supply voltage of 5.5V (worst-case test conditions for SEL); a constantly rotating input angle was supplied (5kHz input frequencies) and the device configured for 16-bit operation. Three beam runs were performed under the conditions listed in Table I. A latchup condition would have been manifested as an increase in power supply current, IDD. No increase in IDD was observed, even for the highest LET tested in Table I. This result suggests the design is latchup immune to an LET of at least 100 MeV-cm²/mg. Future testing and qualification on a modified design will confirm this result on multiple devices.

Table I. Latchup Testing Beam Parameters.

Ion	LET(Si) MeV.cm2/mg	Tilt deg	Fluence #/cm2	Comments
I-127	60.10	0	3.137E+06	SEL Test at 125C 5.5V: no latch
I-127	78.57	40.1	2.051E+06	SEL Test at 125C 5.5V: no latch
Au-197	106.46	40.1	2.012E+06	SEL Test at 125C 5.5V: no latch

SEU (Single-Event-Upset) Testing

The SEU testing was divided into two segments: monitoring for upsets in the digital output latches, and monitoring for heavy-ion effects (most likely single-event transients) in the analog circuitry of the RDC (the closed-loop converter system). In both cases the device was powered at 4.5V and operated at room temperature (again, worst-case conditions for this type of test). For the digital tests, a constant angle value was loaded into the device output register. After loading the output registers, the part was inhibited (placed in a static mode) so that the output latches would not respond to any further input angle changes (perhaps from upsets in the operating converter system). Any changes detected on the output by continuously reading the output word were counted in software and reported as SEU errors. Similarly, for the analog tests, a constant-angle input signal dynamically drove the RDC while the beam was on. In this case, the part was not inhibited. Again, busy pulses were counted and output state changes were recorded. The system was observed to be free of noise prior to turning on the beam (there were no spurious busy pulses).

Static-Mode Upset Results

Four beam runs were performed with Au-197 at a 40-degree incidence angle ($LET_{EFF}=106.46$ MeV-cm²/mg) to a fluence of 10^7 ions/cm². Observations indicated a dependence on the initial input (resolver) angle in the nature of the upset response. We chose four input angles, generating 16-bit output words of hexadecimal FFFF, 5555 (alternating 1's and 0's), 8000 (180°), and 0000. The output latches were all DICE [1] latches and were not expected to upset, however, by our detection technique, we noticed in the FFFF case, multiple bit changes in a single "event". However, in the 5555 case, only single bits changed in each event. In both cases, "1" bits always cleared to the "0" state. The event counts were low, and the events seemed to occur very rapidly after the onset of the beam. After the first few seconds, no further events were detected for the remainder of the beam run (2-4 minutes). The results are shown in detail in Table II. In the 1000 case, the MSB cleared immediately, and no other events were detected. No upsets were observed in the 0000 input case. The part always resumed resolving to the correct input angles once the inhibit condition was removed following the termination of the beam exposure.

Table II. Inhibited-Mode Upset Test Results.

Run #54: Input=HEX FFFF

Upset	Output	HEX	MSB	LSB
0	65535	FFFF	11111111	11111111
1	255	00FF	00000000	11111111
2	13	000D	00000000	00001101
3	0	0000	00000000	00000000

Run #55: Input=HEX 5555

Upset	Output	HEX	MSB	LSB
0	21845	5555	01010101	01010101
1	21829	5545	01010101	01000101
2	21828	5544	01010101	01000100
3	21824	5540	01010101	01000000

Run #56: Input=HEX 8000

Upset	Output	HEX	MSB	LSB
0	32768	8000	10000000	00000000
1	0	0000	00000000	00000000

These results are not yet fully understood. The symmetric nature of the circuitry involved in the DICE latches does not suggest an upset mechanism which is preferential to the zero logic state. In fact, the nature of the circuitry does not suggest an upset mechanism at all. However, a new resolver input angle appears to get written to the output register each time a new answer is generated in the inhibited mode of operation during beam exposure. Analog input signals were used during the test which would result in answers with a large number of zeros (e.g., FFFF changing to 0000). An SEU event in the register strobe circuitry (a small number of gates) would then possibly cause the output register to assume a new state preferring mostly zeros under those conditions where the strobe was abnormally narrow (an SEU strike). Analysis of this nature suggests experiment conditions which might further refine understanding of the device (or experiment) behavior (i.e., radically changing the input angle signal after the output registers are loaded and inhibited). Further investigations will be performed at the next SEE investigation experiment.

Dynamic-Mode Upset Results

When the part was operated in the dynamic mode with the inhibit condition removed, many busy pulses (counted with a pulse counter) and many output state changes were observed. Several busy pulses or output state changes may occur in response to a single charge-transfer event from the ion beam. These “upsets” are always temporary, because the part always resolves back to the input resolver angle. (In the following results, any output state change was counted as an upset while the part dynamically looped to re-resolve on the input angle signal. We even counted the “zero-bit” magnitude changes where the output angle returned to its original input value.) A small sample of the output results is shown in Table III. The first column is a running count of the number of

Table III. Sample output record during an uninhibited-mode beam exposure.

Upset	Output	HEX	MSB	LSB	Change
0	43690	AAAA	10101010	10101010	0
1	43685	AAA5	10101010	10100101	-5
2	43683	AAA3	10101010	10100011	-7
3	43684	AAA4	10101010	10100100	-6
4	43689	AAA9	10101010	10101001	-1
5	43690	AAAA	10101010	10101010	0
6	43689	AAA9	10101010	10101001	-1
7	43688	AAA8	10101010	10101000	-2
8	43687	AAA7	10101010	10100111	-3
9	43688	AAA8	10101010	10101000	-2
10	43689	AAA9	10101010	10101001	-1
11	43690	AAAA	10101010	10101010	0
12	43691	AAAB	10101010	10101011	1
13	43692	AAAC	10101010	10101100	2
14	43703	AAB7	10101010	10110111	13
15	43699	AAB3	10101010	10110011	9
16	43693	AAAD	10101010	10101101	3
17	43692	AAAC	10101010	10101100	2
18	43691	AAAB	10101010	10101011	1
19	43695	AAAF	10101010	10101111	5

changes observed in the output. The output is listed as a decimal count in the second column, where one count is $1/2^{16} \times 360^\circ \times 3600'' \approx 20''$ of arc. The HEX and MSB/LSB columns illustrate which bits of the output registers are changing in response to transients in the closed-loop feedback system. The last column shows the count-size or magnitude of the change each output state represents relative to the original input value. Note the 0-valued output state changes (lines 5 and 11) are counted as upsets and that multiple bits may change at each counted upset. These bit changes may be either 0-1 or 1-0 transitions. The magnitude of the changes were always small; the largest observed had a count magnitude of 40, or less than $15'$ of arc.

In addition, the upsets were observed to come in spurts, followed by several seconds of quiescence, where the resolver output would remain steady at the input angle reading. Unfortunately, no timing information was recorded during the beam exposure. Nevertheless, a qualitative idea of the resolver response can be gleaned from Figure 1, where the magnitudes of the upsets are plotted in sequence for an entire beam exposure. There is a cyclic behavior, suggesting the action of the feedback loop re-adjusting the output latch registers to match the input-angle signal. All beam runs for each LET value showed similar behavior.

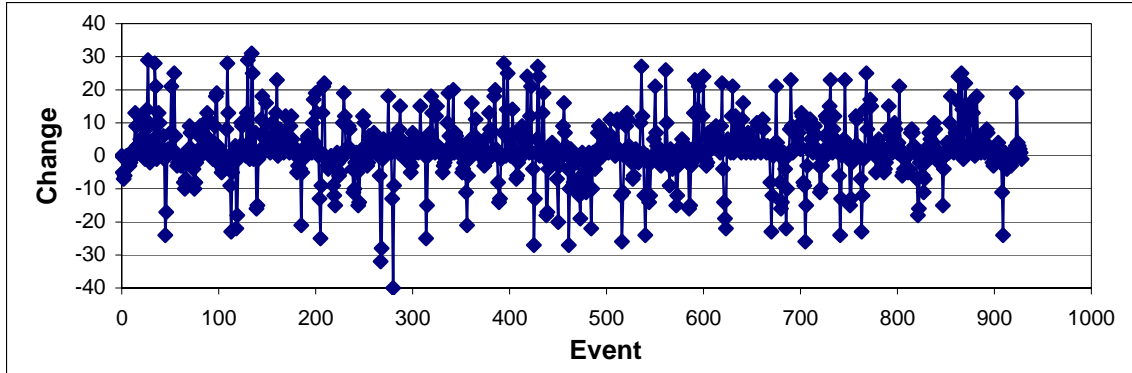


Figure 1. Sequence of upsets observed during a sample beam exposure.

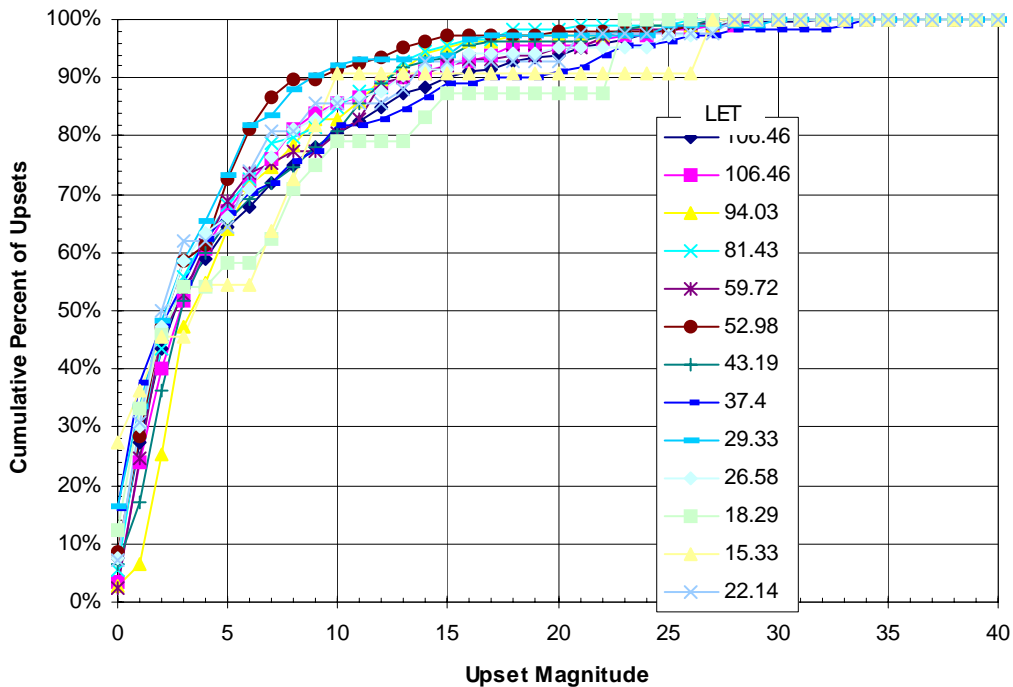


Figure 2. Distribution of upset magnitudes for all LET values.

The distributions of the magnitudes of change (in decimal counts) are shown in Figure 2 for all LET values used in the dynamic mode tests. More than half of the errors are of a count size of 5 or less, and only about 20% are larger than 20 counts. A dependence on LET is not observable in the data of Figure 1 because beam fluence has not been accounted for and each curve is normalized to the total number of upsets for that run (hence the 100% y-axis scale). However, in this representation, the absence of LET dependence implies higher-energy ions are not more likely to cause larger magnitude upsets than do lower-energy ions. This preferential tendency of the ion beams to produce small magnitude changes independent of LET suggests the upsets are caused by transient perturbations in the closed-loop converter system and that these perturbations saturate at a very low LET.

Table IV. Beam parameters and upset results for uninhibited-mode tests.

Run #	Ion	LET(Si) MeV.cm ² /mg	Tilt deg	Fluence #/cm ²	Output Upsets	CrossSec cm ²	Busy Pulses	CrossSec cm ²
58	Au-197	106.46	40.1	1.629E+06	928	5.698E-04		
61	Au-197	106.46	40.1	2.659E+05	111	4.174E-04	615	2.313E-03
62	Au-197	94.03	30	1.252E+05	105	8.385E-04	446	3.562E-03
63	Au-197	81.43	0.1	2.239E+05	112	5.003E-04	515	2.300E-03
64	I-127	69.45	30.7	1.652E+05	100	6.053E-04	537	3.250E-03
65	I-127	59.72	0.1	2.349E+05	128	5.450E-04	754	3.210E-03
66	Br-80	52.98	45.1	1.591E+05	105	6.600E-04	409	2.571E-03
67	Br-80	43.19	30	3.093E+05	109	3.524E-04	511	1.652E-03
68	Br-80	37.40	0	3.449E+05	110	3.189E-04	764	2.215E-03
69	Ni-58	29.33	25	3.790E+05	101	2.665E-04	434	1.145E-03
70	Ni-58	26.58	0	4.392E+05	105	2.391E-04	580	1.321E-03
73	Cl-35	22.14	58	1.464E+06	41	2.800E-05	225	1.537E-04
71	Cl-35	18.29	50.1	2.134E+06	23	1.078E-05	165	7.733E-05
72	Cl-35	15.33	40.1	4.996E+06	10	2.002E-06	73	1.461E-05
76	Cl-35	13.61	30.5	1.011E+08	0	0.000E+00	0	0.000E+00
74	Cl-35	11.73	0.1	9.368E+06	0	0.000E+00	0	0.000E+00
75	Cl-35	11.73	0.1	1.001E+08	0	0.000E+00	0	0.000E+00

A list of the test conditions for these beam exposures are listed in Table IV. The output upset counts listed are the total number of output state changes (cumulative of all count sizes). In addition, the number of busy pulses recorded from the pulse counter during the beam exposure are listed. These two kinds of upsets led to two different cross-section values, with there being a larger cross-section for busy pulses than for output changes. These upset cross-sections are quite well correlated, with the busy-pulse cross-section being about 5× larger than the output-change cross-section. The correlation between the two cross-sections is seen in Figure 3. Figure 4 plots each cross-section as a function of LET, showing the upset threshold (around 14 MeV-cm²/mg) and the saturation cross sections. Both datasets are fitted with Weibull curves with the same shape parameters, but differing in saturation cross-section. The Weibull fit takes the following form,

$$\sigma \left(1 - \exp \left[- \left(\frac{LET - 14}{20} \right)^{2.4} \right] \right)$$

where the LET is in MeV-cm²/mg and the cross section σ is 5.9×10^{-4} cm² for the output changes and 2.9×10^{-3} cm² for the busy pulses. The larger cross-section of busy pulses suggests that not all output state changes were being captured by the data-read loop of the computer. We found the data-read loop to be as long as 2ms while writing the new output state to disk. Each busy pulse should correspond with an output state change, and so it represents the worst-case error rate for the RDC.

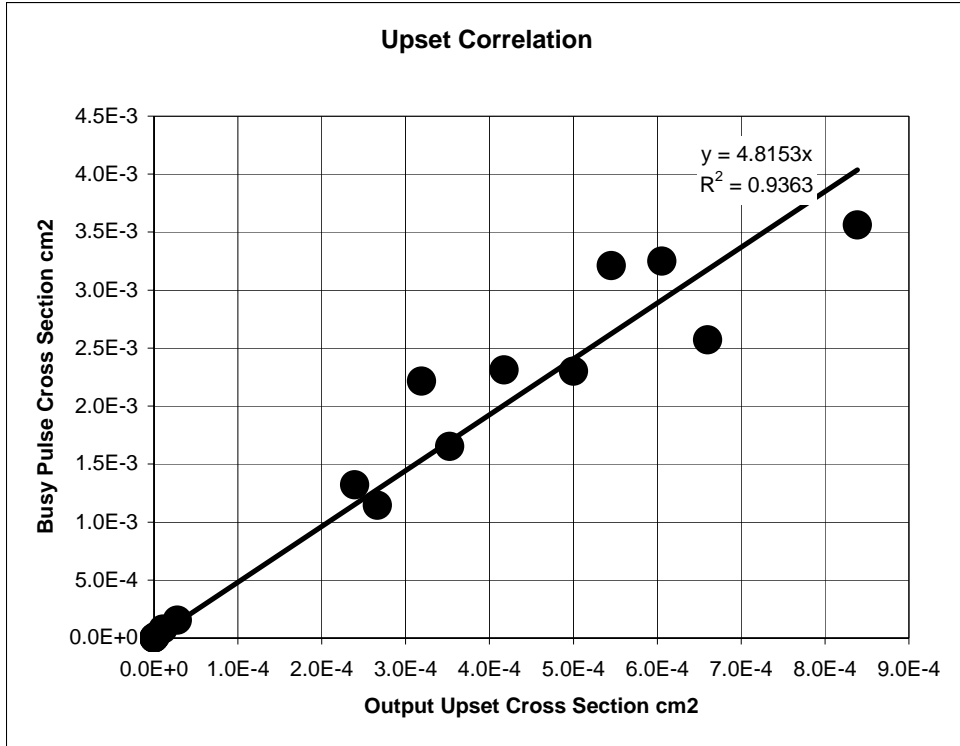


Figure 3. Output changes correlate with busy pulse counts.

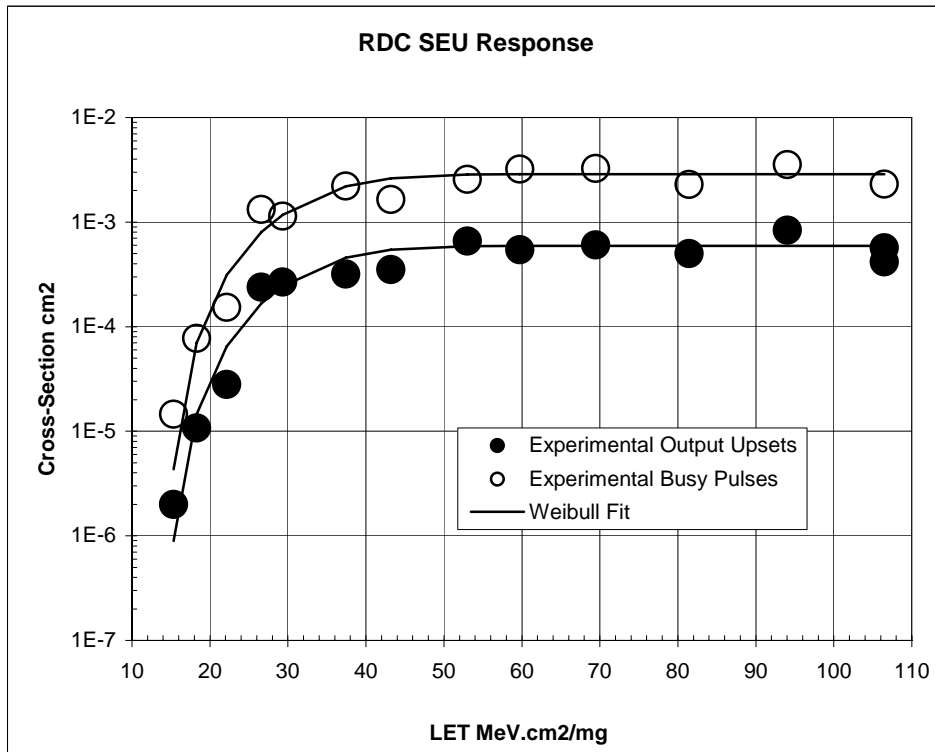


Figure 4. Cross-section vs. LET curves for output changes and busy pulses.

Now, we can account for the fluence of each beam in analyzing the output upset cross-section according to the upset magnitudes. Figure 5 shows the data of Figure 2 normalized to the saturation cross-section (total output upsets/beam fluence) of Figure 4. Now the LET dependence of the upset magnitudes can clearly be seen. If we plot the normalized cross-sections as a function of LET for some of the various upset magnitudes, we obtain cross-section curves similar to those of Figure 4. Such curves are plotted in Figure 6. Note that the curve for the upset bin 40 (the cumulative count of all upsets with magnitude 40 and less) is the same curve plotted as the filled symbols in Figure 4. Of course, for upset bins of magnitude less than 40, the cross-section values are lower. Since each curve in Figure 5 has nearly the same shape and is simply shifted to higher cross sections with higher LET, we conclude only the frequency of events increased with LET, but not the magnitude.

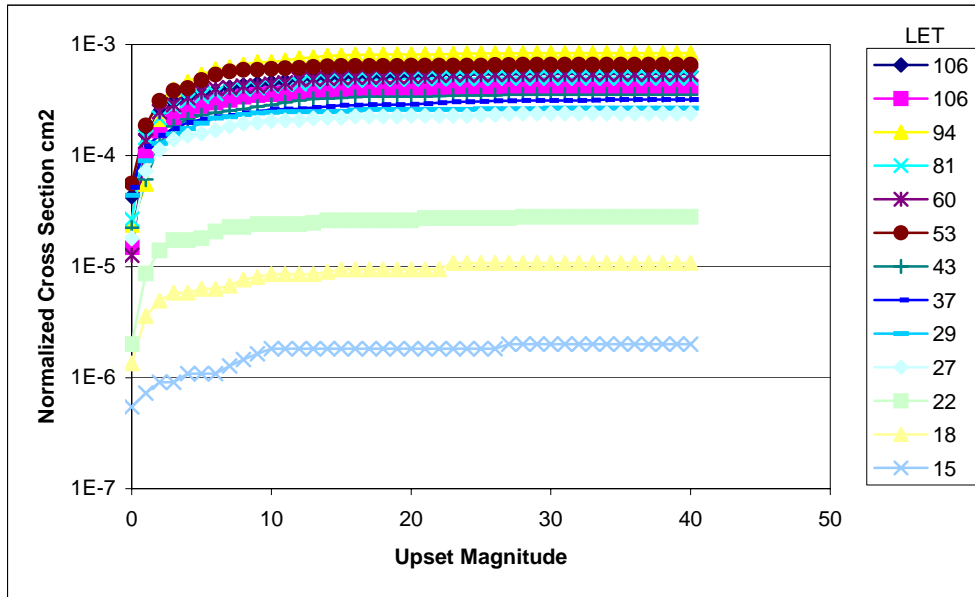


Figure 5. Upset magnitude dependence on LET.

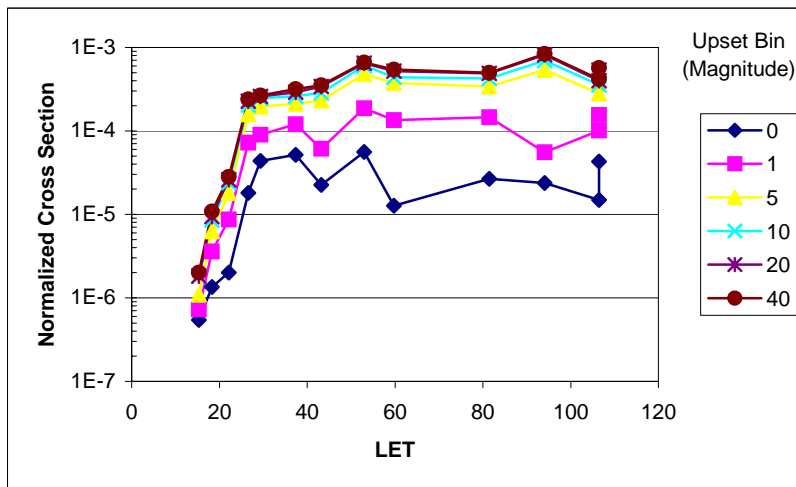


Figure 6. Cross-section curves for various upset-magnitude bins.

Error Rate Calculations

The data above were used with CREME96 [2] to calculate upset rates. For these calculations, we assumed the worst-case geosynchronous orbit and 100 mils of Al shielding. We considered the flux of ions across the full range of atomic number (1 to 92) and assumed the RPP cross-section to be equivalent to the saturation cross-section of each error type considered. [3] Finally, we assumed a critical depth of 2 μ m. From these assumptions, we calculated rates of 1.5×10^{-3} busy pulses/device/day and 3×10^{-4} output upsets of 15' minutes or less per device per day due to interplanetary heavy-ion bombardment. The rates for smaller magnitude upsets (say 1 LSB) are about 20-30% of the total upset rate. Since the busy-pulse counts represent the worst-case output-state change frequency, the heavy-ion environment of a geosynchronous orbit might be responsible for a single output state change (1 busy pulse) once in every couple of years, according to these predictions. It is unclear how these error rates will depend on the resolution mode (10, 12, or 14 bit) of the RDC; the 16-bit mode might be thought worst case because of the extreme sensitivity to small upsets. However, the lower resolution modes have higher bandwidth, and might therefore be more sensitive to transients in the linear amplifiers. These effects will be investigated in future tests of a redesigned RDC.

Summary

Heavy-ion beam irradiation testing of the RDC has provided evidence that the current design is latchup immune (as expected) to an LET of at least 100 MeV-cm²/mg. The dynamic upset rate of the RDC in a geosynchronous orbit has been calculated to be on the order of 10^{-3} upsets/device/day with an error magnitude of 15' of arc or less. The RDC (as designed) should be suitable for most space applications with little system design impact for mitigating single event effects.

References

- [1] T Calin, M. Nicolaidis, R. Velazco, "Upset Hardened Memory Design for Submicron CMOS Technology", IEEE Trans. Nucl. Sci., Dec. 1996, pp. 2874-2878.
- [2] A.J. Tylka, James H. Adams, Jr., Paul R. Boberg, Buddy Brownstein, William F. Dietrich, Erwin O. Flueckiger, Edward L. Petersen, Margaret A. Shea, Don F. Smart, and Edward C. Smith, "CREME96: A Revision of the Cosmic Ray Effects on Micro-Electronics Code", IEEE Transactions on Nuclear Science, 44, 2150-2160 (1997).
- [3] E.L. Petersen, J.C. Pickel, J.H. Adams, Jr., and E.C. Smith, "Rate Prediction for Single Event Effects -- a Critique," IEEE Transactions on Nuclear Science NS-39, No. 6, pp. 1577-1599, December 1992.

Aeroflex Plainview assumes no responsibility for the information contained in this application note, and no license or rights are granted by implication or otherwise in connection therewith.

Please visit our WEB site at www.aeroflex.com for the latest information.

Plainview Contact: Steve Friedman 516-752-2456

steve.friedman@eroflex.com

PLAINVIEW, NEW YORK

Toll Free: 800-THE-1553
Fax: 516-694-6715

INTERNATIONAL

Tel: 805-778-9229
Fax: 805-778-1980

NORTHEAST

Tel: 603-888-3975
Fax: 603-888-4585

SE AND MID-ATLANTIC

Tel: 321-951-4164
Fax: 321-951-4254

WEST COAST

Tel: 949-362-2260
Fax: 949-362-2266

CENTRAL

Tel: 719-594-8017
Fax: 719-594-8468

www.aeroflex.com info-ams@eroflex.com



As we are always seeking to improve our products, the information in this document gives only a general indication of the product capacity, performance and suitability, none of which shall form part of any contract. We reserve the right to make design changes without notice. All trademarks are acknowledged. Parent company Aeroflex, Inc. ©Aeroflex 2003.



Our passion for performance is defined by three attributes represented by these three icons: solution-minded, performance-driven and customer-focused